Plant Physiol. (1975) 55, 917–922

The Interaction between Osmotic- and Pressure-induced Water Flow in Plant Roots[1]

Received for publication October 5, 1974 and in revised form January 16, 1975

EDWIN L. FISCUS
Department of Botany, Duke University, Durham, North Carolina 27706

ABSTRACT

This paper presents a general model for coupled solute and water flow through plant roots based on the thermodynamics of irreversible processes. The model explains in a straightforward manner such experimentally observed phenomena as changes in root resistance, increased solute flux, and apparent negative resistance, which have been reported for root systems under the influence of a hydrostatic pressure gradient. These apparent anomalies are explained on the basis of the interaction between the osmotic and hydrostatic driving forces and the well known "sweeping away" or dilution effect. We show that with a constant hydraulic conductivity the only features necessary to explain these phenomena are some type of membrane or membranelike structure and a mechanism for actively accumulating solutes.

A recurring problem in plant-water relations research in recent years has been the apparent change in resistance to water flow through root systems with changes in transpiration rate or applied hydrostatic pressure. These changes are not observed by all workers nor do they appear to occur in all species studied (2). Also, most of the apparent changes were observed at relatively low rates of transpiration.

Most of the early work was aimed at elucidating the influence of water flow on the rates of salt uptake and transport to the shoot. Russell and Barbar (12), Brouwer (1), and Kramer (8) all review the early literature on this subject. In this paper, we will confine ourselves to consideration of the interaction of solute and water transport in detached root systems and the consequent nonlinear relationship between water flow and driving force. As far as we are aware, only two laboratories have produced sufficient relevant data that bear directly on this question and for this reason we will draw heavily from the experiments of Lopushinsky (9, 10) and Mees and Weatherley (11). They both demonstrated clearly that under the influence of an applied hydrostatic pressure gradient the resistance to water flow in detopped tomato root systems did change. The relationship between applied pressure and flow rate was nonlinear to the extent that there were changes of from 5- to 20-fold in the slope of the force-flux curve over a pressure range of only 2 bars.

Thus far, no adequate explanation has been advanced to account for these changes in root resistance. This paper, using a simple membrane system, demonstrates changes in water conductivity with increasing hydrostatic pressure without any actual change in the hydraulic conductivity coefficient. It is proposed that a similar system, if operating in a root, would produce many of the effects which have been observed.

MATERIALS AND METHODS

Consider, in Figure 1, a simple semipermeable membrane of unit area separating two compartments. The outside compartment (superscript o) is very large and well stirred throughout, while the inside compartment (superscript i) is also well stirred but limited in size. Although limited in size, the inside compartment is open-ended so that water flow through the membrane is unconstrained by any back pressure. The membrane is assumed to be rigid, capable of moving solutes against a potential gradient, and for the present, totally impermeable to solutes (reflection coefficient $\sigma = 1$, and solute permeability $\omega = 0$). The actual mechanism of solute accumulation is unimportant for our purposes, but we do assume throughout that it operates at a constant rate and is unaffected by volume flow, applied pressure, or internal or external solute concentrations. We further specify that there is only one solute species present, and since we do not include electrical forces, it is assumed to be a nonelectrolyte.

In the absence of a hydrostatic pressure gradient ($P^o = P^i$), such a system will develop a steady state concentration difference between the inside and outside compartments and water will flow across the membrane in response to this gradient. Assuming ideality of the solutions, the osmotic pressure on the inside will be

$$\pi^i = RTC^i \quad (1)$$

where R is the gas constant in ml atm deg^{-1} mole^{-1}, T is the absolute temperature, and C^i is the internal concentration in mole cm^{-3}. At the steady state it is clear that C^i is dependent on the ratio of the entry rates of the solutes and water, and we may write

$$C^i = J_s/J_w \quad (2)$$

where J_s and J_w are the solute and water fluxes, respectively. Since the membrane is ideal, the only solute flux will be active and we may replace J_s with an active uptake term J_s^* in mole cm^{-2} sec^{-1}. We may also assume that the water flow J_w is equal to the totol flow of volume J_v in cm sec^{-1}. Thus we have

$$C^i = J_s^*/J_v \quad (3)$$

The volume flow in our system, when subjected to both osmotic and hydrostatic pressure gradients, is

$$J_v = L_p(\Delta P - \Delta\pi) \quad (4)$$

Again, assuming ideal solutions and substituting from equation

[1] This work was supported by National Science Foundation Grant GB-36643.

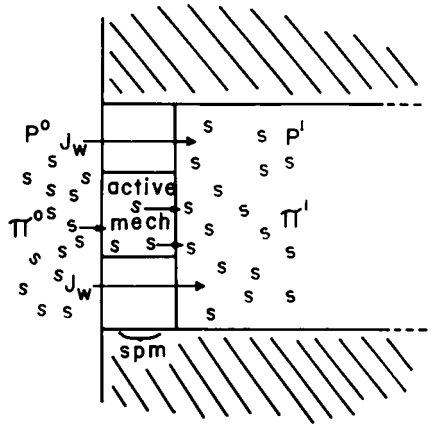

FIG. 1. The model system. A semipermeable membrane (spm) containing an active solute uptake mechanism capable of moving solutes against a potential gradient.

3 for C^i, we get

$$J_v = L_p\left[\Delta P - RT\left(C^o - \frac{J_s^*}{J_v}\right)\right] \quad (5)$$

which may be multiplied by J_v and rearranged to the standard quadratic form

$$J_v^2 + J_v L_p(\pi^o - \Delta P) - L_p RT J_s^* = 0 \quad (6)$$

which is easily solved for J_v by the quadratic formula.

For much of our discussion, however, it will be more convenient to use equation 5 solved for ΔP. That is

$$\Delta P = \frac{J_v}{L_p} + RT\left(C^o - \frac{J_s^*}{J_v}\right) \quad (7)$$

This form is more convenient because the apparent resistance to hydrostatic pressure flow is simply the slope of the force-flux curve when the relevant force is given as the dependent variable. The apparent resistance is therefore the first derivative of ΔP with respect to J_v.

$$R^a = \frac{d\Delta P}{dJ_v} = \frac{1}{L_p} + \frac{RTJ_s^*}{J_v^2} \quad (8)$$

where R^a is the apparent resistance. We use the term apparent resistance to avoid confusing this term with any of the thermodynamic inverse coefficients (see Kirkwood [6] for a discussion of inverse coefficients). We shall see later that the apparent resistance, under certain circumstances, approaches very closely the thermodynamic hydraulic resistance term. For lack of a better term, we will use apparent resistance even though what we are describing is a true resistance.

To explore the influence of the parameters in equation 5 on the shape of the force-flux curve, we solved equation 6 for J_v then equation 8 for R^a over a range of values for L_p, J_s^*, π^o, and ΔP. The ranges of the variables used were determined by values found in or estimated from the literature. The ranges used are in Table I. The calculations were done with a FORTRAN program on an IBM 370 165 computer.

RESULTS AND DISCUSSION

Equation 6 clearly shows that in the system under consideration volume flow is nonlinear with respect to ΔP. However, of much greater interest is equation 8 which shows the dependence of the apparent resistance on the flow rate. Here we see that the apparent resistance is made up of two components. The first part, which depends only on the hydraulic conductivity coefficient, remains constant with flow, while the second part decreases with the inverse square of the flow rate. The over-all effect is shown in Figure 2, where the effect of the variable term in equation 8 is clarified. As J_v increases, the variable term tends to disappear and the apparent resistance approaches the limiting value of $1/L_p$. At relatively high flow rates, the apparent resistance approaches a value consistent with the irreversible thermodynamic relationship between straight and inverse coefficients in a system consisting of only one flow and its conjugate force (*i.e.*, $R_i = 1/L_i$).

The inset in Figure 2 is redrawn from Lopushinsky (9) and clearly illustrates the similarities between his experimental data and our theoretical curves. Flow and concentration units are not specified in the inset because the original units were not given in terms of absorbing area and are not directly comparable in magnitude. However, there are a number of very interesting points of comparison.

Both curves indicate a positive flow rate at $\Delta P = 0$. This is, of course, the well known phenomenon of root pressure exudation. When external pressure is applied to the system, we see that in both cases the apparent resistance is initially high but that it gradually decreases to what appears to be a nearly constant value. If our theory is correct, or nearly so, we can expect the limiting slopes of these lines to have the value $1/L_p$.

Comparison of the concentration curves is also interesting in that in both cases the internal concentration, or osmotic pressure, is above ambient at $\Delta P = 0$. Increased flow through the application of pressure brings about a decrease of C^i below ambient concentrations and appears to approach some limiting value. In the case of our simple system that limiting value would be zero at infinite pressure. It is possible, although unlikely, that Lopushinsky's curve approaches that same limit. In any case, C^i in his experiments dropped to approximately 10% of C^o at a pressure of 2 atm, whereas our curve drops to 10% at about 2.5 atm ΔP. Also, Mees and Weatherley (11) reported that the concentration of the pressure exudate from their tomtato root systems often fell to a small fraction of the external medium. The actual numerical values are unimportant for our purposes, and

Table I. *Range of Parameters Used for Generating Curves in Figures*

Parameter	Range	Increment
L_p (cm sec^{-1} atm^{-1})	$1(10^{-8})$ to $5(10^{-5})$	1, 2, 5
J_s^* (mole cm^{-2} sec^{-1})	$1(10^{-13})$ to $5(10^{-10})$	1, 2, 5
π^o (atm)	1 to 10	0.25 atm
ΔP (atm)	1 to 5	0.5 atm

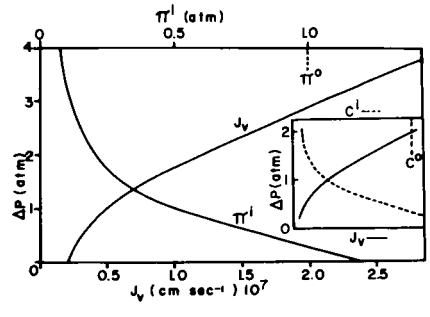

FIG. 2. Relationship between applied pressure, volume flow rate, and internal osmotic pressure for the model system. $J_s^* = 0.1(10^{-11})$ mole cm^{-2}sec^{-1}; $L_p = 0.1(10^{-6})$ cm sec^{-1}atm^{-1}; $\pi^o = 1$ atm. The inset is redrawn from Lopushinsky (9).

it is sufficient to observe that flow increases in a nonlinear manner and that $C^i > C^o$ at low J_v and $C^i \ll C^o$ at high J_v.

It is clear from Figure 2 and equation 5 that the cause of the nonlinear response of water flow with respect to pressure is due simply to the decrease of one driving force ($\Delta\pi$) with increases in the other (ΔP). This point is further illustrated in Figure 3. Here we show the total inwardly directed driving force acting on the membrane as a function of the applied external pressure. This relationship is shown at two levels of external osmotic pressure and three levels of hydraulic conductivity. The dashed line is drawn where the total force is equal to the applied pressure (*i.e.* where $\Delta\pi = 0$).

We can easily see that at low pressures, hence low flow rates, the osmotic component dominates. At moderate pressures $\Delta\pi$ tends toward zero then goes positive as C^i falls below C^o. At high pressures when the slope of the curve approaches the slope of the dashed line, the curve is offset from the dashed line by an amount very close to π^o. Extrapolation of these lines backward to the abscissa shows an intercept equal to π^o. This result is true only for the ideal membrane presently under discussion.

The degree of nonlinearity as shown by Figure 3 is influenced to a great extent by π^o as well as L_p and J_s*. In order to clarify this relationship, we calculated the parameter R_o/R_l for comparison at different levels of L_p, J_s*, and π^o. This parameter is the ratio of R^a when $\Delta P \rightarrow 0$, to the limiting value $1/L_p$. This ratio gives an indication of the degree of nonlinearity to be expected under a given set of conditions. Figures 4 and 5 show the

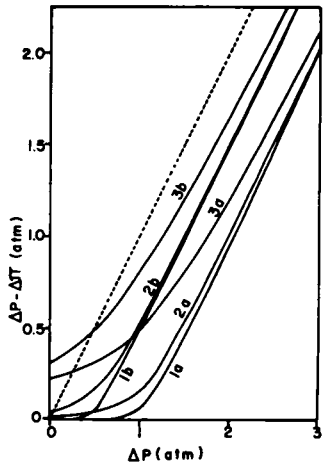

FIG. 3. Total inwardly directed driving force as a function of applied pressure. The dashed line is the equipotential line (where the total force is equal to the applied pressure, $\Delta\pi = 0$). Lettering on figure as follows: π^o: a = 1 atm, b = 0.5 atm; L_p: 1 = $0.5(10^{-5})$, 2 = $0.5(10^{-6})$, 3 = $0.5(10^{-7})$ cm $sec^{-1}atm^{-1}$.

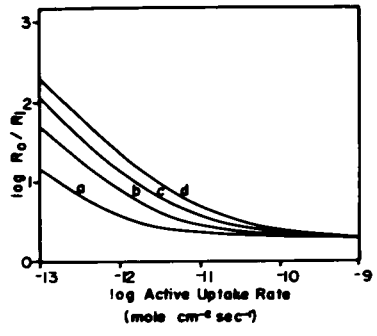

FIG. 4. Degree of curvature of the force-flux curves as influenced by J_s* and π^o. $L_p = 0.5(10^{-6})$ cm $sec^{-1}atm^{-1}$. Lettering on figure as follows: π^o: a = 0.25, b = 0.5, c = 0.75, d = 1.0 atm.

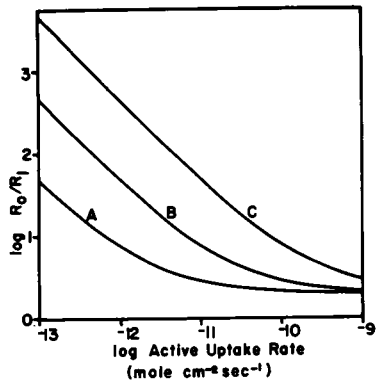

FIG. 5. Influence of J_s* and L_p on the degree of curvature of the force-flux curves. π^o = 0.5 atm. L_p: A = $0.5(10^{-6})$, B = $0.5(10^{-5})$, C = $0.5(10^{-4})$ cm $sec^{-1}atm^{-1}$.

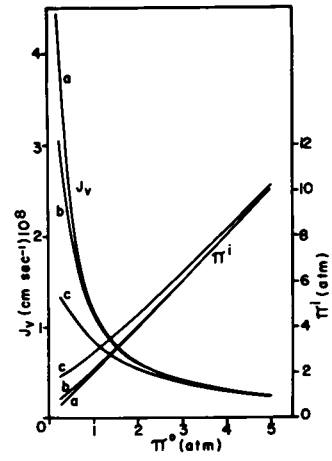

FIG. 6. Effect of increasing external osmotic pressure, π^o, on J_v according to equation 4. J_s* = $0.1(10^{-11})$ mole $cm^{-2}sec^{-1}$. Lettering on figure indicates L_p: a = $0.1(10^{-5})$, b = $0.1(10^{-6})$, c = $0.1(10^{-7})$ cm $sec^{-1}atm^{-1}$.

results of this type of comparison. It is evident that the degree of nonlinearity, as indicated by R_o/R_l increases with (*a*) increasing L_p, (*b*) increasing π^o and (*c*) decreasing J_s*. The apparent changes in resistance then can be quite dramatic under the appropriate conditions.

Another interesting feature of our system is shown in Figure 6 where we see the effects of π^o on π^i and J_v in the absence of a hydrostatic pressure gradient. Here again it is important to note that J_s* is assumed constant. In this case, the constraint is reasonable, since we can use a relatively nonpermeant agent as an osmoticum and keep the external concentration of the actively accumulated species constant. The result is predictable, that is, as the flow rate was decreased by the external osmoticum, the internal concentration increased and flow was maintained at a positive level. Clearly, with a membrane capable of actively accumulating solutes against a potential gradient, it would be impossible to completely stop steady state flow merely by adding external osmotica. This effect was noted by Klepper (7), but she used permeant solutes to raise π^o so the results are not readily compared.

One further interesting point should be made concerning the ideal system. Since the flux equation is nonlinear, the effect of changing L_p is not as clear as it would appear from equation 3 even when $\Delta P = 0$. The relationship between flow rate and hydraulic conductivity is seen to be highly nonlinear (Fig. 7). In addition, the flow rate of our system is very insensitive to

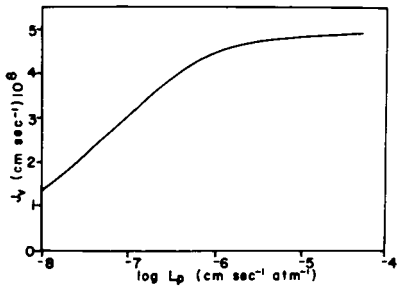

FIG. 7. Effect of changing L_p on the flow rate at $\Delta P = 0$. $J_s^* = 0.1(10^{-11})$ mole cm^{-2}sec^{-1}. $\pi^o = 0.5$ atm.

changes in L_p since, as we can see, an increase of L_p over four orders of magnitude results in only a 4-fold increase in the flow rate under these conditions.

Thus far we have been dealing with ideally semipermeable membranes. Although we can account for the nonlinearity of the force-flux relationship frequently observed in root systems by what is commonly referred to as the "sweeping away" or dilution effect, our system is still linear with respect to the total inwardly directed driving force ($\Delta P - \Delta\pi$). This result leaves unanswered the problem observed by Mees and Weatherley (11) in their early work, where they observed the occurrence not only of a nonlinear flow with respect to pressure, but also with respect to the total inwardly directed driving force. They suggested that part of this effect may have been due to the differences between the osmotic and hydrostatic permeabilities to water and that a given gradient of osmotic pressure might not be as effective in moving water as an equal gradient of hydrostatic pressure. This is essentially the effect produced by membranes that are less than ideally semipermeable and is presently described by the reflection coefficient σ. Obviously, our ideal system is inadequate to explain these observations, so it was necessary to modify our initial equations to account for the nonideal behavior.

When the membrane is less than ideal, equation 3 is no longer precise. In addition to the active component of uptake J_s^*, the total flux consists of two additional terms, a diffusive and a drag component. For such a system, we may write after Katchalsky and Curran (4) for the total solute flux

$$J_s = C_s(1 - \sigma)J_v + \omega\Delta\pi + J_s^* \tag{9}$$

where C_s is the "average concentration" on both sides of the membrane, σ is the reflection coefficient having values $0 < \sigma \leq 1$, ω is the coefficient of solute permeability, and the other terms are as before. The first term on the right represents the solute flux caused by the solvent drag or entrainment effect where solute molecules or ions are carried along with the flow of water. The second term is purely diffusive in nature, and the third term is dependent on metabolic energy. Considering an actively exuding root system in the absence of applied pressure, at the steady state we usually find that the concentration of the xylem exudate is significantly higher than the external medium. In this case, it is clear that the diffusive term will tend to drive solutes through the membrane toward the outside, and it is also clear that the inwardly directed solute fluxes predominate. A full discussion of the influence of the diffusive term on the total solute flux is beyond the scope of this paper, but the appropriate equations are presented in the appendix. Our calculations (unpublished) indicate that for values of ω for some electrolytes of interest in plant membranes (see values collected by Tyree [13]) the diffusive term may be regarded as small compared to the active and drag components without affecting the basic sense of the following discussion. We will then simply ignore the diffusive term. We will return later to consider briefly the situation under applied pressure where moderate flow rates may bring about a reversal of the osmotic gradient, that is, where $\pi^o > \pi^i$.

For the purpose of further analysis, we therefore write for the total solute flux in mole cm^{-2} sec^{-1}

$$J_s = \bar{C}_s(1 - \sigma)J_v + J_s^* \tag{10}$$

To cast equation 10 in a more useful form, we need to consider further the average concentration $\bar{C}_s$ which is defined as

$$C_s = \frac{\Delta C_s}{\Delta \ln C_s} \tag{11}$$

Within limits, we can approximate this term by use of a logarithmic series (*cf.*, Katchalsky and Curran [4] page 118) and provided C^o, C^i is near to unity we may write

$$C_s \approx \frac{C^o + C^i}{2} \tag{12}$$

The greater the deviation of C^o, C^i from unity the larger will be the error in the approximation. We have determined that for $0.3 \leq C^o\ C^i \leq 3$, the approximating error does not exceed 10% in the direction that the approximation is larger than the actual value of C_s. Accepting this approximation as adequate, we may insert equation 10 into equation 2 and solve for C^i

$$C^i = \frac{C^o(1 - \sigma)J_v + 2J_s^*}{J_v(1 + \sigma)} \tag{13}$$

which may be substituted into a modified form of equation 4 containing σ [*i.e.*, $J_v = L_p(\Delta P - \sigma\Delta\pi)$] and

$$J_v = L_p\left(\Delta P - \frac{2\sigma^2\pi^o}{1 + \sigma}\right) + \frac{2\sigma L_p RTJ_s^*}{J_v(1 + \sigma)} \tag{14}$$

which is again quadratic in J_v and has the property that when $\sigma = 1$ it reduces to equation 5.

Solving for ΔP and following our previous procedure for calculating R^a, we get

$$R^a = \frac{d\Delta P}{dJ_v} = \frac{1}{L_p} + \frac{2\sigma RTJ_s^*}{(1 + \sigma)J_v^2} \tag{15}$$

which is the same as equation 8 except that it contains a correction for the solvent drag effect.

To answer our question of whether the reflection coefficient could account for the apparent anomalous behavior observed by Mees and Weatherley (11), we generated flow curves using equations 13 and 14 at various levels of σ. The relationship between flow rate and the total inwardly directed driving force (Fig. 8) is obviously strongly dependent on the reflection coefficient. We can see that for ideal membranes ($\sigma = 1$) the relationship is a straight line, as before, but as the selectivity decreases the nonlinearity increases, and we eventually arrive at a situation where the force-flux relationship takes on a negative slope at low flow rates. This apparent "negative resistance" region is simply the result of two changing differentially effective driving forces. We see, therefore, that it is possible to explain the apparent "negative resistance" effect in a straightforward manner and the data of Mees and Weatherley (11) are not anomalous after all.

It should also be noted that the horizontal lines in Figure 8 connect points of equal hydrostatic pressure, and it is of interest that at constant pressure, a change of σ has relatively little effect on flow rate. In fact, a change in σ may result in an increase or decrease of flow rate.

Another property of our nonideal system that is often noted in plant root systems is the increase in solute flux with increases in flow or applied pressure. The results of calculations of solute flux rates with pressure, using equations 2, 13, and 14 are shown

in Figure 9. Since we have assumed in these calculations that L_p and J_s^* are constant, the increase in solute flux with pressure can only be the result of the solvent drag effect. This is not to say that increases in J_s^* with pressure or flow are not possible, only that they are not necessary to explain increased solute flux in our system. Further, examination of the assumptions used in arriving at equation 10 reveals that we should expect an increase in the total solute flux J_s on a purely physical basis. This increase in J_s results from the diffusive term ω which we ignored in writing equation 10. The effect of ω, as we noted earlier, is that at low flow rates the osmotic gradient is negative in the direction of volume flow and tends to reduce J_s. However, at higher pressures where the dilution effect is sufficient to reduce C^i below ambient, the effect of the diffusive term progresses from loss through zero, to additive. The net result of this would be to increase solute flux at moderate and high flow rates somewhat more than our present calculations would predict. In both the cases of diffusion induced decreases in J_s at low flow rates, and increases in J_s at higher flow rates, the effect of ω should be more pronounced in relatively coarse less selective membranes because of the relationship between σ and ω (5).

A brief word concerning the experiments of Jensen *et al.* (3) is in order here. They demonstrated in their experiments a strictly linear force-flux relationship for water flow in tomato and sunflower roots and stems. Their experimental system was such that the root system was not provided with a source of solutes so that J_s^* was necessarily zero. In this case, equation 15 reduces to $R^a = 1/L_p$ = constant, and flow would be expected to be linear. Their experiments therefore are consistent with our model.

CONCLUSIONS

We have presented in this paper a simple membrane system incorporating a generalized active solute uptake mechanism. It is shown that such a system can adequately account for the nonlinear relationship between flow rate and applied pressure in plant root systems noted by some workers and indeed can, if the membrane is less than ideal, account for apparent negative resistance characteristics. In this regard, it should be mentioned that what we have designated in some figures as the total inwardly directed driving force ($\Delta P - \Delta\pi$) is actually the parameter called the total water potential difference ($\Delta\psi$) by plant scientists. Mees and Weatherley observed experimentally, and we now confirm on theoretical grounds, that water flow between phases is not necessarily a linear function of the total water potential difference. Additionally, the system exhibits increased solute flux with increased pressure or flow rate which has been noted by many workers. The increased solute flux in the system is due to two components—the solvent drag effect and enhanced diffusion brought about by the internal dilution effect.

The values chosen for the various root parameters in our calculations cover wide ranges of conditions. We have attempted to cover the very wide range of values for these parameters found in the literature and have not attempted to assign any "most likely value" status to any of these. The choices of the values used for the figures were occasionally somewhat arbitrary in order to accentuate a particular point, but we have tried to stay within what we considered reasonable bounds in doing so. In this connection, it must be recalled that the nature of the functional root membrane is not well defined, and it may or may not have properties similar to a typical plant plasmalemma. Also, these properties probably vary along the root axis. One would expect the conductivity in the older portions of the root to decrease considerably as suberization progresses, but the advent of secondary growth could alter the functional membrane and make it quite leaky. In the latter case, σ would drop well below its value in the younger portions of the root, while L_p would be expected to become quite large. It was for these reasons that we included what may appear to be excessively low values for σ and very high values for L_p.

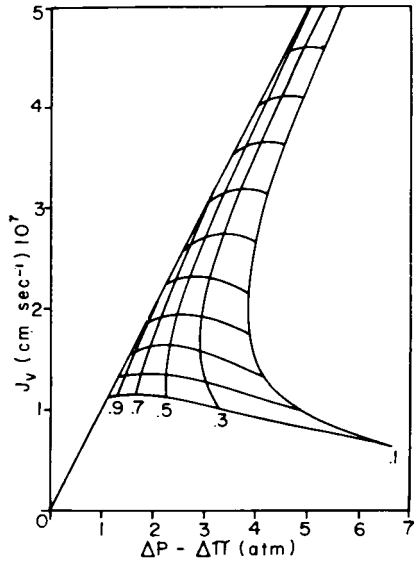

FIG. 8. Effect of reflection coefficient on the total force-flux curve illustrating the negative resistance region. The straight line is $\sigma = 1$. $J_s^* = 0.1(10^{-10})$, $L_p = 0.1(10^{-6})$, $\pi^o = 1$. The horizontal lines connect points of equal hydrostatic pressure. The numbers on the curves denote the reflection coefficients.

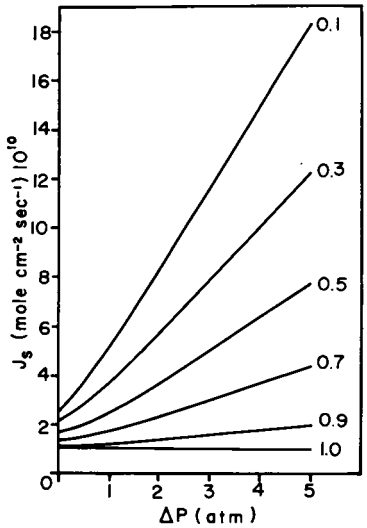

FIG. 9. Total solute flux as influenced by applied pressure and reflection coefficient. The numbers on the curves denote the reflection coefficients. $J_s^* = 0.1(10^{-11})$, $L_p = 0.1(10^{-6})$, $\pi^o = 1$.

The flow rates which result from the use of this model (Figs. 2 and 6–8) seem somewhat low compared to rates reported in the literature, both from this laboratory and others. The flow rates are simply the result of the values used for the parameters in the various equations, and if J_v seems low, it may be only a reflection of our lack of knowledge concerning the true values of the parameters L_p, σ, and J_s^*, and more importantly, their distribution in the root. Therefore, care must be taken in applying the equations we have developed in this paper to roots or root systems if only for geometrical considerations. We have dealt with a flat membrane of uniform properties and not a cylindrical system where L_p, σ, and J_s^* may be expected to vary along the axis. Such a cylindrical system would more accurately reflect the

situation in a terminal root segment, but the flat membrane geometry may be used as an approximation to more complex root systems, especially if the basal regions are much less conductive than the apical regions. In this case, the membrane properties could not be thought of as uniformly distributed across the conductive areas, and measured values of L_p, σ, and J_s^* would necessarily reflect some type of "average" conditions.

We have dealt only with nonelectrolyte uptake in this paper and have not tried to simulate a root or root system. It has been our intent only to demonstrate in general terms a possible cause of apparent anomalies in the force-flux relationships of some root systems. This fact is obviously another shortcoming of the model along with the fact that we have considered J_s^* insensitive to external concentrations, which we also know is not accurate, especially in the range of $\pi^o < 1$ atm.

Regardless of these shortcomings, we feel that the model system presented is sufficiently based on fact and consistent with enough experimental data to warrant its further consideration as a general model for coupled solute and water flow through plant roots.

APPENDIX

To arrive at an expression containing the effects of all three solute flux terms—active, drag, and diffusive—we may start from equation 9 of the text. We accept the approximation of $\bar{C}_s$ (equation 12) and will treat ω as a measurable quantity even though it does contain a buried $\bar{C}_s$ term. We therefore write from equation 9

$$J_s = \frac{C^o + C^i}{2}(1 - \sigma)J_v + \omega RT(C^o - C^i) + J_s^* \qquad (16)$$

From the relationship of equation 2 we may divide by J_v and solve for C^i to get

$$C^i = \frac{C^o(1 - \sigma)J_v + 2\omega\pi^o + 2J_s^*}{(1 + \sigma)J_v + 2\omega RT} \qquad (17)$$

Insertion of equation 17 into the modified form of equation 4 containing σ yields

$$J_v = L_p\Delta P - \sigma L_p\pi^o + \sigma L_p RT\left[\frac{C^o(1 - \sigma)J_v + 2\omega\pi^o + 2J_s^*}{J_v(1 + \sigma) + 2\omega RT}\right] \qquad (18)$$

Collecting terms and rearranging to the standard quadratic form gives

$$J_v^2(1 + \sigma) + J_v[2\omega RT - L_p\Delta P(1 + \sigma) + 2\sigma^2 L_p\pi^o] - 2L_p RT(\omega\Delta P + \sigma J_s^*) = 0 \qquad (19)$$

Solving equation 18 for ΔP and taking the first derivative with respect to J_v, we find the apparent resistance as

$$R^a = \frac{d\Delta P}{dJ_v} = \frac{1}{L_p} + \frac{2\sigma RT[2\sigma\omega\pi^o + J_s^*(1 + \sigma)]}{[J_v(1 + \sigma) + 2\omega RT]^2}. \qquad (20)$$

Acknowledgments—I wish to acknowledge the very helpful discussions with Drs. John D. Hesketh and Paul J. Kramer during the early part of this work. Without their help and encouragement, this work would not have been completed.

LITERATURE CITED

1. Brouwer, R. 1965. Ion absorption and transport in plants. Annu. Rev. Plant Physiol. 16: 241-266.
2. Hailey, J. L., E. A. Hiler, W. R. Jordan, and C. H. M. van Bavel. 1973. Resistance to water flow in *Vigna sinensis* at high rates of transpiration. Crop Sci. 13: 264-267.
3. Jensen, R. D., S. A. Taylor, and H. H. Wiebe. 1961. Negative transport and resistance to water flow through plants. Plant Physiol. 36: 633-638.
4. Katchalsky, A. and P. F. Curran. 1965. Nonequilibrium Thermodynamics in Biophysics. Harvard University Press, Cambridge. p. 215.
5. Kedem, O. and A. Katchalsky. 1961. A physical interpretation of the phenomenological coefficients of membrane permeability. J. Gen. Physiol. 45: 143-179.
6. Kirkwood, J. G. 1954. *In:* H. T. Clarke, ed., Ion Transport Across Membranes. Academic Press, New York. p. 119.
7. Klepper, B. 1967. Effects of osmotic pressure on exudation from corn roots. Aust. J. Biol. Sci. 20: 723-735.
8. Kramer, P. J. 1969. Plant and Soil Water Relationships: A Modern Synthesis. McGraw-Hill, New York. p. 244.
9. Lopushinsky, W. 1964. Effects of water movement on ion movement into the xylem of tomato roots. Plant Physiol. 39: 494-501.
10. Lopushinsky, W. 1961. Effect of water movement on salt movement through tomato roots. Nature 192: 994-995.
11. Mees, G. C. and P. E. Weatherley, 1957. The mechanism of water absorption by roots. I. Preliminary studies on the effects of hydrostatic pressure gradients. Proc. R. Soc. London Ser. B 147: 367-380.
12. Russell, R. S. and D. A. Barber. 1960. The relationship between salt uptake and the absorption of water by intact plants. Annu. Rev. Plant Physiol. 11: 127-140.
13. Tyree, M. T. 1970. The symplast concept: a general theory of symplastic transport according to the thermodynamics of irreversible processes. J. Theor. Biol. 26: 181-214.